PROTEINS: Structure, Function, and Genetics 29:401–416 (1997)

INVITED REVIEW

Mechanisms of Signaling and Related Enzymes

Albert S. Mildvan*
Department of Biological Chemistry, The Johns Hopkins School of Medicine, Baltimore, Maryland

ABSTRACT **Most enzymes involved in cell signaling, such as protein kinases, protein phosphatases, GTPases, and nucleotide cyclases catalyze nucleophilic substitutions at phosphorus. When possible, the mechanisms of such enzymes are most clearly described *quantitatively* in terms of how associative or dissociative they are. The mechanisms of cell signaling enzymes range from ≤8% associative (cAMP-dependent protein kinase) to ~50% associative (G protein Giα1). Their catalytic powers range from $10^{5.7}$ ($p21^{ras}$) to $10^{11.7}$ (λ Ser-Thr protein phosphatase), usually comparable in magnitude with those of nonsignaling enzymes of the same mechanistic class. Exceptions are G proteins, which are 10^3- to 10^5-fold poorer catalysts than F1 and myosin ATPases. The lower catalytic powers of G proteins may be ascribed to the absence of general base catalysis, and additionally in the case of $p21^{ras}$, to the absence of a catalytic Arg residue, which interacts with the transition state. From kinetic studies of mutant and metal ion substituted enzymes, the catalytic powers of cell signaling and related enzymes can be rationalized quantitatively by factors contributed by metal ion catalysis (≥10^5), general acid catalysis (~$10^{3\pm1}$), general base catalysis (~$10^{3\pm1}$), and transition-state stabilization by cationic and hydrogen bond donating residues (~$10^{3\pm1}$). Proteins 29:401–416, 1997.** © 1997 Wiley-Liss, Inc.

Key words: nucleophilic substitution at phosphorus; associative mechanisms; dissociative mechanisms; transition-state structures; Staphylococcal nuclease; protein kinases; tyrosine kinases; G proteins; F1 ATPase; myosin ATPase; phosphoserine-phosphothreonine protein phosphatases; phosphotyrosine protein phosphatases

INTRODUCTION

The field of enzyme mechanisms seeks to explain how enzymes work in terms of the underlying principles of physical organic and coordination chemistry. The goals of this field have been evolving from searches for *qualitative* descriptions of enzyme mechanisms to *quantitative* explanations of the basis of the enormous catalytic powers of enzymes that can accelerate reaction rates by factors as high as 10^{16}-fold.[1,2]

Catalytic power is most simply defined as the ratio of the maximal turnover number of an enzyme-catalyzed reaction (k_{cat}) to the pseudofirst-order rate constant for the same reaction in solution, extrapolated to the same temperature and pH (k_{soln}). This definition relates the half-life of the substrate in the rate-limiting enzyme complex to its half-life in solution.** Intracellular signaling pathways use many enzymes, most of which catalyze nucleophilic substitutions at phosphorus, such as protein kinases and phosphatases, GTP hydrolases, ATP and GTP cyclases, and phospholipases. Exceptions are rhodopsin, which catalytically activates G proteins, and protein methylases and demethylases involved in bacterial chemotaxis. Appropriate mechanistic questions to ask about signaling enzymes are: 1) How do they work? 2) Are their catalytic powers unusually high or low? and 3) How are their rate accelerations achieved? Recent structural and kinetic studies of signaling enzymes, making use of catalytically altered mutants, have begun to provide answers to these questions.

This review focuses on the mechanisms of those signaling enzymes that catalyze nucleophilic substitutions at phosphorus. Table I lists the catalytic powers of well-studied signaling enzymes and com-

**More elaborate definitions of catalytic power compare k_{cat}/K_m values on the enzyme to second-order rate constants of the same reaction in solution. These comparisons require properly determined k_{cat}/K_m values, which are not always available, and present difficulties as to which K_m to use for enzymes with more than one substrate. Second-order rate constants in solution can also be multiple, involving catalysis by H_3O^+, OH^-, and water.

Grant sponsor: National Institutes of Health; Grant number: DK28616.

*Correspondence to: Albert S. Mildvan, Department of Biological Chemistry, The Johns Hopkins School of Medicine, 725 North Wolfe Street, Baltimore, MD 21205.

Received 1 May 1997; Accepted 9 June 1997

pares them with familiar nonsignaling enzymes of the same mechanistic class. With the exception of the slow autophosphorylation catalyzed by the insulin receptor tyrosine kinase, it is clear that protein kinases, both of the serine and tyrosine kinase type, have very high catalytic powers comparable with, or even greater than that of hexokinase. Protein serine or threonine phosphatases also have high catalytic powers comparable with that of alkaline phosphatase, whereas tyrosine phosphatases are an order of magnitude slower. G proteins have very low catalytic powers in hydrolyzing GTP, ranging from 10^3- to 10^5-fold lower than those of F1 and myosin ATPases. A goal of this review is to explain mechanistically the high catalytic powers of protein kinases and phosphatases and the low catalytic powers of G proteins. Such mechanistic information will contribute to our understanding of how such enzymes can be regulated in performing their important biological functions.

MECHANISTIC CONSIDERATIONS

Nucleophilic substitutions at phosphorus have been described in terms of a continuum of mechanisms with two limiting cases, a fully dissociative mechanism that proceeds via a trigonal metaphosphate *intermediate* and a fully associative mechanism that involves a trigonal bipyramidal *intermediate* (Fig. 1A). Between these extremes are mechanisms with no intermediates but with trigonal bipyramidal *transition states*.[3,4] This continuum of mechanisms is best appreciated by considering the *axial distances* from the entering and leaving oxygens to the reaction center phosphorus in the trigonal bipyramidal intermediate or transition state, which measure the extent of bonding of the entering and leaving atoms to phosphorus (Fig. 1B). In a fully dissociative mechanism, the axial P-O distances would both be ≥3.3 Å, the van der Waals sum of phosphorus (1.9 Å) and oxygen (1.4 Å), indicating only contact but no bonding. These long distances would result in a metaphosphate intermediate with an axial bond number of 0 to both the entering and leaving groups. In a fully associative mechanism, the axial bond distances would both be those of covalent single P-O bonds, 1.73 Å in length.[5] Intermediate cases, which are usually found on enzymes, have axial P-O distances between 3.3 and 1.73 Å, indicating transition states with fractional P-O bond numbers between 0 and 1 and mechanisms that are partially associative. A classical S_N2 mechanism would have 0.5 bonds to both the entering and leaving groups in the trigonal bipyramidal transition state. The relationship between bond distance D(n) and fractional bond number (n) has been given by Pauling[5] as

$$D(n) = D(1) - 0.60 \log (n) \qquad (1)$$

in which D(1) is the single bond distance, 1.73 Å for the P-O bond. From Eq. (1), a P-O bond that is half formed would have an axial bond distance of 1.91 Å. Because the leaving group leaves in all mechanisms, *the axial bond number (n) to the entering group in the transition state defines the fractional associativity of the mechanism*. Thus, the S_N2 mechanism could be described as 50% associative. Axial bond distances on enzymes can, in some cases, be estimated from crystal structures of appropriate transition-state analogs or can be inferred from ^{18}O kinetic isotope effects[4] or from linear free-energy relationships.[6]

Upper limits to axial distances in the transition state can be estimated from distances between the entering and leaving atoms in X-ray or NMR-determined structures of ground-state enzyme-substrate complexes, by making the simplifying assumption of a symmetric transition state in which only the [PO_3] moiety has moved to a position equidistant from the entering and leaving atoms. Because this approximation neglects decreases in axial bond lengths due to contraction of the transition state, it tends to underestimate the fractional associativity of a mechanism.

Another mechanistically useful distance obtainable from X-ray or NMR data, which also provides a lower limit to the fractional associativity of a mechanism, is the *reaction coordinate distance*, defined as the distance between the entering atom and the phosphorus undergoing substitution before the reaction has begun.[3,7] Again, assuming that the only motion during the reaction is that of the [PO_3] moiety, a reaction coordinate distance ≥4.9 Å allows room for a nonbonded metaphosphate intermediate in a fully dissociative mechanism.† A reaction coordinate distance <4.9 Å permits new bond formation to the entering atom to occur before old bond breakage to the leaving atom has been completed, thus providing some associative character to the mechanism. The shorter the reaction coordinate distance, the greater the associative character. When the reaction coordinate distance is that of molecular contact (3.3 Å), the distance between the entering and leaving oxygen atoms, if perfectly aligned with the phosphorus, is 5.0 Å. If this distance were to be fixed during the reaction, a symmetric transition state would have axial bond lengths of 2.5 Å to both the entering and leaving atoms, which correspond to fractional bonds of 0.052 to each, from Eq. (1), and to a mechanism that is 5.2% associative or 94.8% dissociative. The value of 5.2% associative is a lower limit because the associativity of a mechanism can be increased by an asymmetric, product-like transition state or by compression in the ground state and/or the transition state.

†The lower limit value of 4.9 Å is derived by adding to the van der Waals contact distance between phosphorus and the entering oxygen (3.3 Å) the value 1.6 Å by which the distance to the leaving oxygen must increase as its covalent bonding distance (1.7 Å) elongates to a van der Waals contact distance (3.3 Å).

A

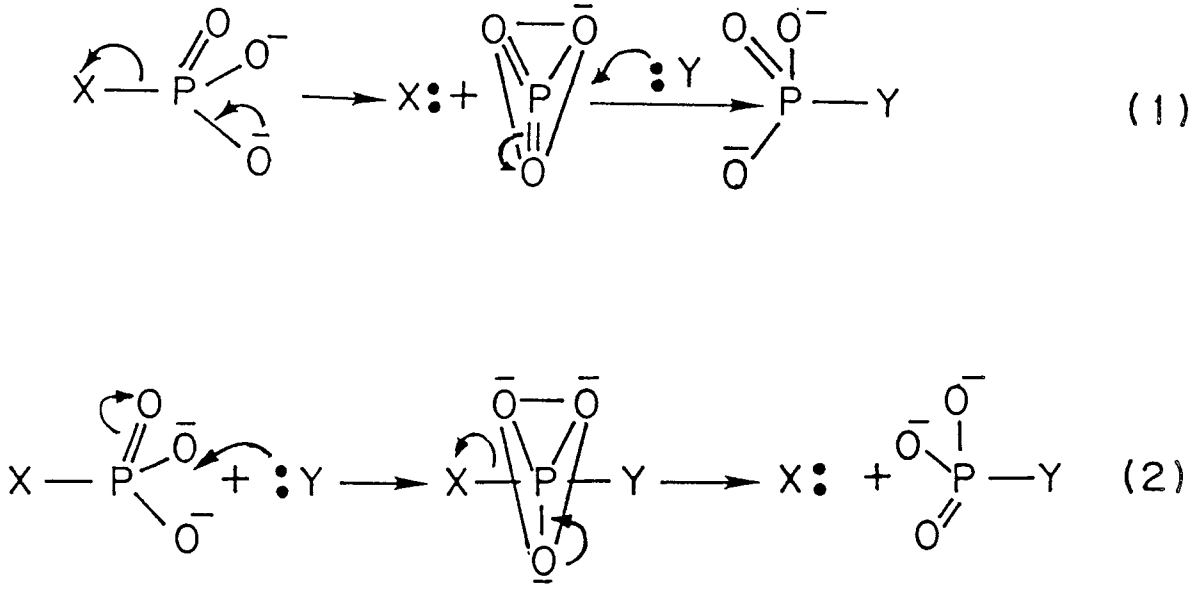

B MECHANISM

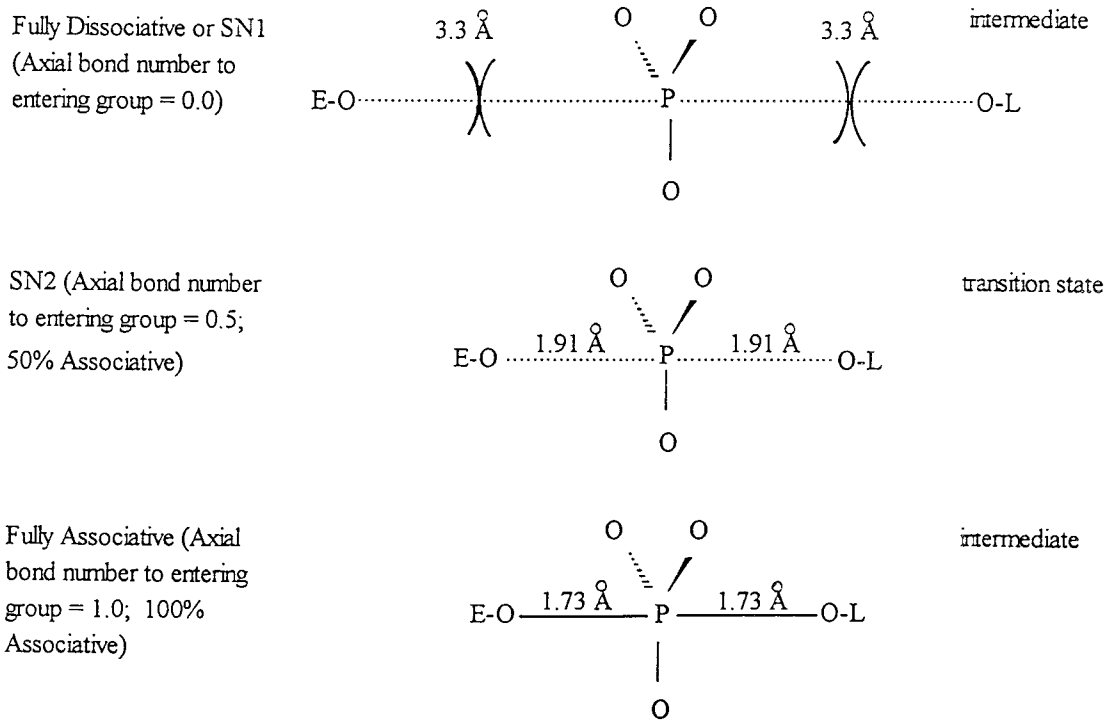

Fig. 1. Mechanisms of nucleophilic substitution at phosphorus.[3,4,7] **A:** Limiting fully dissociative mechanism with a metaphosphate intermediate (1), and a fully associative mechanism with a phosphorane intermediate (2). **B:** Dimensions of intermediates and transition states in various mechanisms of substitution at phosphorus.

The ability to quantitate the fractional associativity of a mechanism would dispel much of the confusion and apparent disagreement in the literature resulting from such vague qualitative statements as "an associative mechanism with a dissociative transition state," "an associative mechanism with an exploded transition state," or "a dissociative mechanism with some associative character."

STAPHYLOCOCCAL NUCLEASE

One of the most powerful enzymes known, which catalyzes nucleophilic substitution at phosphorus with a catalytic power of 10^{16}-fold, is this nonsignaling nuclease.[1] A phosphodiesterase, this widely studied enzyme can contribute to a quantitative understanding of the mechanisms of other enzymes that catalyze nucleophilic substitutions at phosphorus, including those involved in cell signaling. Staphylococcal nuclease requires Ca^{2+} to catalyze the hydrolysis of phosphodiester linkages found in DNA and RNA. A combination of X-ray diffraction and NMR spectroscopy has been used to determine the structures of the ground-state E-M^{2+}-dAdT substrate complex[8] and of the E-M^{2+}-pdTp complex,[9] which mimics the charge of the transition state, but not its trigonal bipyramidal geometry. The ground-state structure (Fig. 2A) indicates that the enzyme-bound metal ion coordinates both the attacked phosphoryl group and the attacking water (or hydroxyl ion). The reaction coordinate distance of 4.3 Å is $<$4.9 Å, indicating a mechanism with some associative character. Contraction of the reaction center in the transition-state complex is indicated by a 1.4 Å decrease in the metal-phosphorus distance from 4.1 to 2.7 Å[10] and by a change from monofunctional to bifunctional hydrogen bonding of the phosphate by both Arg-35 and Arg-87.[8,9] Such contraction of the axial distance to the entering water oxygen, which cannot be quantitated because of the tetrahedral geometry of pdTp, would increase the associative character of the mechanism.

The attacking water (or hydroxyl ion) is oriented and/or deprotonated by Glu-43 which is positioned to accept a hydrogen bond and appears to function as a general base. Arg-87 is positioned to protonate the leaving 5′-oxygen, thus serving as a general acid. Arg-35 provides additional electrophilic catalysis, donating a hydrogen bond to a phosphoryl oxygen in the ground state. Both Arg-35 and Arg-87, by becoming bifunctional hydrogen bond donors in the transition state, provide transition-state stabilization and explain why lysines at these positions, which cannot act as bifunctional hydrogen bond donors, result in mutants that are 10^4-fold less active.[11]

From the effects on k_{cat} of metal ion substitution for Ca^{2+} and of single and double mutations of catalytic residues, quantitative contributions of each to catalysis may be estimated. Thus, metal ion catalysis by Ca^{2+} contributes a factor of $\geq 10^5$, general acid-base catalysis by Arg-87 and Glu-43 together contribute 10^6, and transition-state stabilization by Arg-35 contributes 10^5 to catalysis, consistent with the overall catalytic power of 10^{16}-fold.

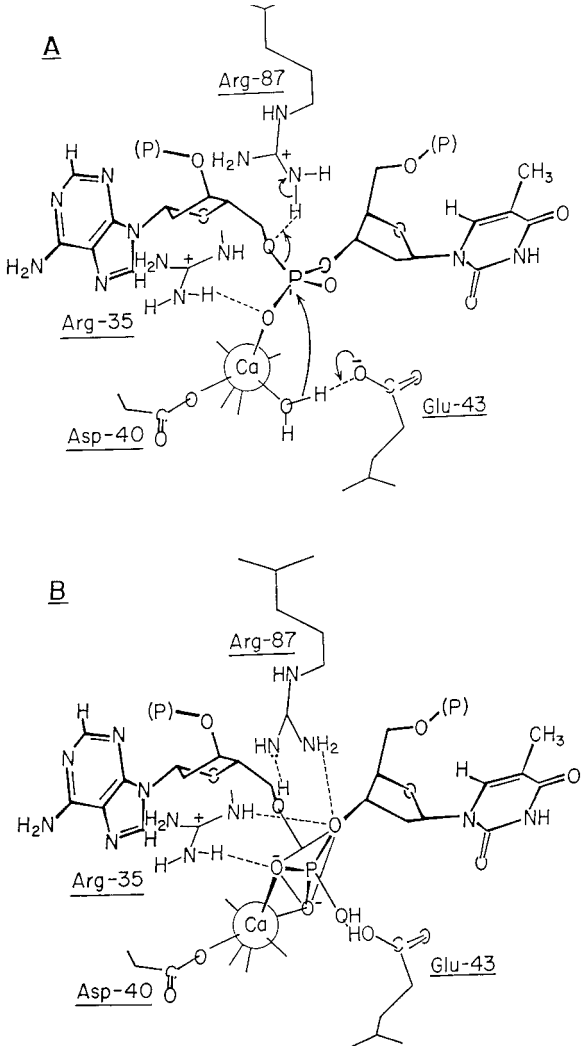

Fig. 2. Staphylococcal nuclease mechanism (**A**) and transition-state structure (**B**) for the hydrolysis of dTdA, based on NMR and X-ray studies[8,9] and on the kinetic effects of mutations.[1,11]

The quantitative paradigm provided by Staphylococcal nuclease has been used to explain the lower catalytic powers of the 3′,5′-exonuclease of DNA polymerase I ($10^{12.5}$) and of ribozymes (10^{12}), which lack general base catalysis, resulting in catalytic powers comparable with that of the E43S mutant of Staphylococcal nuclease ($10^{12.6}$) in which the general base has been removed.[12]‡ It also may explain the

‡In these systems, the two active-site arginines of Staphylococcal nuclease are replaced by a second divalent cation that is positioned to perform the same functions. With Mg^{2+}-dependent ribonuclease H, the double mutation to arginines of aspartate and glutamate metal ligands results in a highly active enzyme that no longer requires Mg^{2+}, supporting the catalytic equivalence of two arginines with a divalent cation on nuclease enzymes.[89]

TABLE I. Catalytic Powers and Mechanisms of Signaling and Mechanistically Related Enzymes

Enzyme	k_{non} (sec^{-1})[83–85]	k_{cat} (sec^{-1})	k_{cat}/k_{non}	% Associative
cA-Kinase[27]	4.7×10^{-9} (23°)	500.	10^{11}	≤8.4
Tyr-Kinase (VFPs)[78]	5.8×10^{-9} (24°)	38.	$10^{9.8}$	
(Src)[77]	6.5×10^{-9} (25°)	52.	$10^{9.9}$	
(Insulin Rcptr)[80] *	4.7×10^{-9} (23°)	0.038 (Auto-Phos.)	$10^{6.9}$	
	4.7×10^{-9} (23°)	12.5 (Peptide-Phos.)	$10^{9.4}$	
(Hexokinase, mitoch.)[81]	1.4×10^{-8} (30°)	123.	10^{10}	
(Staph. nuclease) (pH 7.4)[1]	5.7×10^{-14} (24°)	>95.	$>10^{15.2}$	
Giα1 GTPase[40,46,82]	2.2×10^{-9} (20°)	0.04	$10^{7.3}$	52
Transducin[42,83]	3.8×10^{-9} (23°)	0.05	$10^{7.1}$	36
Goα-GAP GTPase[49]	2.2×10^{-9} (20°)	14.0	$10^{9.8}$	
RAS (wild type)[45]	2.2×10^{-9} (20°)	0.0011	$10^{5.7}$	
RAS (Q61E)[46]	2.2×10^{-9} (20°)	0.022	$10^{7.0}$	
(F1-ATPase, mitoch.)†	3.8×10^{-9} (23°)	180.	$10^{10.7}$	
(Myosin ATPase)[37,84]	2.6×10^{-9} (21°)	160.	$10^{10.8}$	13
λ-Ser/Thr Pase (pH 7.8)[61]	4.45×10^{-9} (30°)	2006.	$10^{11.7}$	
Tyr-Pase (Yersinia)				
(pH 7.0)[75]	4.45×10^{-9} (30°)	34.2	$10^{9.9}$	21
(pH 5.0)[75]	3.07×10^{-7} (30°)	1230.	$10^{9.6}$	
(Alk Pase, *E. coli*) (pH 8.0)[56,85]	8.92×10^{-10} (20°)	100.	$10^{11.0}$	40–68

*R.A. Kohanski, personal communication, 1997.
†Y.H. Ko and P.L. Pedersen, personal communication, 1996.

low catalytic power of a type I topoisomerase in the DNA strand cleavage step (10^9) because this step lacks metal ion catalysis.[13]

PROTEIN KINASES

From an analysis of the complete yeast genome, it has been found that this simplest of eukaryotes has no less than 113 identifiable protein kinase genes, constituting 2% of its proteins,[14] thus emphasizing the importance of protein phosphorylation in cell signaling and metabolic regulation. Among the most thoroughly studied of signaling enzymes is the cAMP-dependent protein kinase or cA-kinase, which phosphorylates Ser or Thr residues in appropriate amino acid sequences.[15,16] The catalytic power of this enzyme (i.e., the catalytic subunit) in the phosphoryl transfer step, 10^{11}-fold, is very high, greater by an order of magnitude than that of hexokinase, a typical kinase (Table I). Early kinetic data and structural studies by NMR,[3,17] and more recently by X-ray crystallography have been reviewed extensively.[18] Crystal structures of the quaternary $E(Mn^{2+})_2$-ATP-Ala peptide complex in the closed, active conformation located the two divalent cations, one activating and the other partially inhibitory, at the active site (Fig. 3)[18,19] in agreement with their earlier positioning by NMR methods.[20] The activating divalent cation is β,γ coordinated by ATP in the Δ configuration,[21] and the partially inhibitory divalent cation bridges the enzyme to the α- and γ-phosphoryl groups of ATP.[18–20] The 20-residue inhibitory Ala-peptide, containing the sequence -RRNAI- is an analog of the substrate peptide that contains the sequence -RRASI- and that can be phosphorylated on serine. Such peptides assume an extended conformation at the active site of the enzyme as found by NMR[22,23] and by X-ray diffraction.[19,24] As found by NMR with parallel kinetic assays, in solution the enzyme-bound ATP shows a high-antiglycosyl torsional angle ($\chi = 78 \pm 10°$) when the enzyme is fully active, which decreases to a low-antiglycosyl torsional angle ($\chi \sim 30°$) as activity is lost.[25] The crystalline enzymes show low-antiglycosyl conformations for bound ATP ($\chi = 32°$[18]; $\chi = 47°$[19]), suggesting that the enzyme may have lost some activity during the prolonged collection of X-ray data.

By superimposing the crystal structure of the product E-phosphopeptide complex onto that of the "substrate" $E(Mn^{2+})_2$-ATP-Ala peptide complex, it was found that, in the overall reaction, only the transferred phosphoryl group moved, by 1.5 Å, very close to the value of 1.6 Å assumed in deriving the lower limit distance of 4.9 Å for a dissociative mechanism.† The reaction coordinate distance on cA-kinase between the entering oxygen atom and the γ-phosphorus of ATP, estimated in the crystalline state by superimposing the "substrate" $E(Mn^{2+})_2$-ATP-Ala peptide complex onto the abortive $E(Mn^{2+})_2$ADP-Ser peptide complex, was 3.05 ± 0.2 Å.§ Another estimate from model building based on the X-ray structure of the doubly inhibited [E-ADP-N-P—Ala peptide] complex is 2.7 Å.[19] Within experimental error, this reaction coordinate distance suggests molecular contact (3.3 Å) or possibly compression of the entering Ser-oxygen and the γ-P of ATP before the reaction has begun, consistent with a mechanism with some associative character. From the ground-state distance between the entering and leaving oxygens (4.75 Å),[18] assuming a symmetric

§S.S. Taylor, personal communication, 1997.

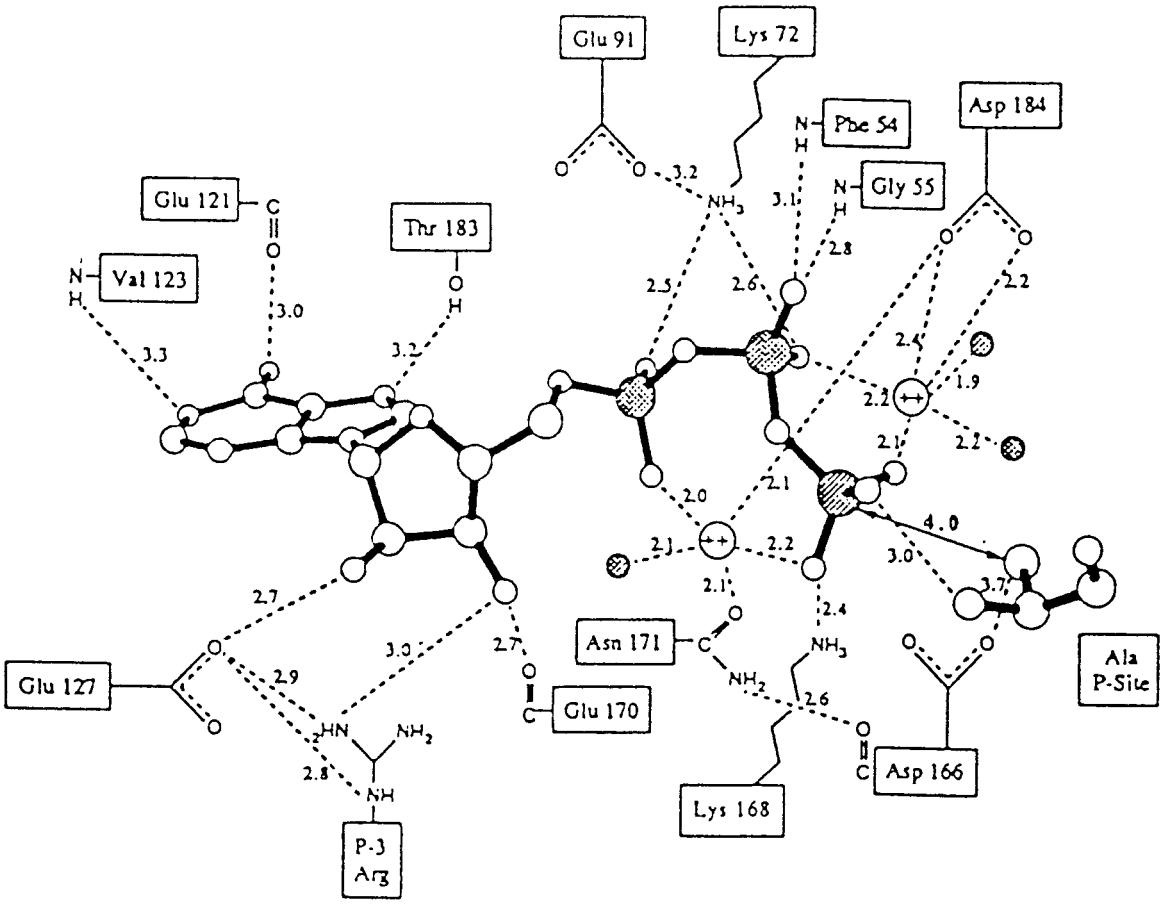

Fig. 3. cAMP-dependent protein kinase active site. Divalent cations and residues that interact with ATP and the inhibitory peptide are shown, based on X-ray data.[18]

transition state, an axial bond number of 0.084 to the entering oxygen is calculated as described above with Eq. (1), corresponding to a mechanism that is 8.4% associative (or 91.6% dissociative). A much longer reaction coordinate distance between the entering oxygen and the γ-P (5.3 ± 0.7 Å) was obtained indirectly by NMR measurements of distances from active-site metals on the nucleotide to the Ser-Cβ methylene protons of the peptide substrate LRRASLG.[26] This distance may be too long because it required the use of AMPPCP, a competitive analog of ATP. The true reaction coordinate distance likely lies between 3.05 and 5.3 Å, in accord with a mechanism with ≤8.4% associative character (Table I).

Residues that contribute to the 10^{11}-fold catalytic power of cA kinase, as judged by the crystal structure of the closed, active conformation (Fig. 3)[18] and by the effects of mutations,[28] include Asp-166, which is positioned to deprotonate and/or orient the entering Ser-OH of the substrate and possibly to orient and activate the γ-phosphoryl group of ATP for substitution. Mutation of Asp-166 to Ala in the yeast enzyme[28] results in a $10^{2.5}$-fold loss of activity, suggesting a corresponding contribution to catalysis. Lys-72, positioned by Glu-91, activates the departure of the ADP leaving group, contributing a factor of $10^{2.9}$, as judged by the effects of its mutation to Ala. Lys-168, by neutralizing charge, promotes entry on ATP contributing a factor of $10^{1.7}$. The activating divalent cation, which neutralizes charge, orients, and polarizes the γ-phosphoryl group, contributing a factor of $\geq 10^{2.5}$ to catalysis, as judged by the effects of mutating the ligand, Asp-184, which positions the metal, to Ala. Assuming all of these effects to be multiplicative (i.e., that their contributions to $\Delta G^{\neq}$ are additive), they contribute at least $10^{9.6}$ to catalysis. Because metal ion catalysis probably has been underestimated by at least 10^2 (see above), the 10^{11}-fold catalytic power of cA kinase can be rationalized easily. Of course, it remains to be shown that the effects of $\Delta G^{\neq}$ of mutating the catalytic residues are indeed additive.

The homologous and structurally related tyrosine kinase of the insulin receptor, with a catalytic power of $10^{9.4}$ (Table I), has residues corresponding to Asp-166, the general base, and Lys-72, which activates the departure of the leaving group. Lys-168,

which facilitates attack at Pγ is conservatively replaced by Arg.[29] These residues, together with the minimal factor of $\geq 10^{2.5}$ for metal ion catalysis, would, if additive, predict a catalytic power of $\geq 10^{9.6}$ for the insulin receptor tyrosine kinase and for tyrosine kinases in general, closely approximating those that are found (Table I). The 10-fold lower catalytic powers of the most active *tyrosine* kinases, compared with the cA-*serine* kinase, may result from suboptimal substrates, or alternatively from the 10^5-fold greater basicity, hence nucleophilicity, of serine alkoxide over phenoxide. If the latter is correct, a β-nucleophilicity of $\log 10/\log 10^5$ or ~0.2 would be operative, which is reasonable for a mechanism with a small amount of associative character.[4,30] A directly measured β-nucleophilicity for a tyrosine kinase of ≤0.08 has recently been reported.[30a]

Before it can phosphorylate exogenous substrates, the insulin receptor tyrosine kinase first must be activated by autophosphorylation of endogenous tyrosine residues. In the inactive, open conformation, one of these endogenous tyrosines, Tyr-1162 of the activation loop is hydrogen bonded (2.6 Å) to Asp-1132, which corresponds to Asp-166, the general base of cA kinase, thus preparing this tyrosine for autophosphorylation and occluding the active site to exogenous substrates.[29] The ATP site also is occluded partially by Phe-1151, a conserved residue that overlaps with the adenine binding site, and by the activation loop that blocks the α- and β-phosphoryl binding sites.[29] Another catalytic deficiency of the inactive, open conformation is the long distance (12.4 Å) between the residues corresponding to Lys-72 and Asp-166 of cA kinase. Because these residues come from different domains, this distance measures the openness of the active site (Fig. 3). In the inactive, open conformation of cA kinase complexed with an inhibitory protein, this distance is 11.2 Å, and it decreases to 7.8 Å in the active, closed complex $E(Mn^{2+})_2$ATP-Ala peptide.[18] These numerous catalytic deficiencies of the inactive conformation of the insulin receptor tyrosine kinase can explain readily the $10^{2.5}$-fold slower rate of its autophosphorylation. Presumably, they are corrected by an extensive conformation change triggered by the autophosphorylation.

The Tyr- or Ser-substrate specificities of protein kinases appear to be determined partly by electrostatic interactions of enzyme residues with substrate residues preceding or following the target residue. With cA kinase, anionic residues of the enzyme interact with cationic residues of the substrate, a typical substrate being LRRASLG.[31] With tyrosine kinases, the charge types for the enzyme and substrate are reversed, a typical substrate being poly-(Glu,Tyr) 4:1.[30] The high sensitivity of the K_m value of this substrate to ionic strength effects with the Csk tyrosine kinase is consistent with such electrostatic interactions.[30]

G PROTEINS AND ATPASES

Unlike typical ATPases, such as mitochondrial F1 ATPase or myosin ATPase with catalytic powers of $10^{10.7}$ and $10^{10.8}$, respectively, cell signaling GTPases or G proteins have much lower catalytic powers, ranging from $10^{5.7}$ ($p21^{ras}$) to $10^{7.3}$ (Giα1 GTPase; Table I). The X-ray structure of F1 ATPase[32,33] and mutagenesis studies of the enzyme from *Escherichia coli*[34–36] can be used to rationalize its high catalytic power. In the asymmetric structure of F1 ATPase solved by Abrahams et al.,[32] a water molecule is positioned near the γ-phosphorus of enzyme-bound Mg^{2+} AMPPNP at a reaction coordinate distance of 4.04 Å, suggesting a mechanism with some associative character. For the mechanistically related ATPase reaction catalyzed by myosin, which has a comparable catalytic power in the hydrolytic step (Table I), two transition-state structures are available, a trigonal bipyramidal E-ADP-O-VO_3^{2-}-OH_2 complex and a square bipyramidal E-ADP-O-AlF_4^{2-}-OH_2 complex. Although both complexes show very similar axial bond lengths, the vanadate complex has a more appropriate overall geometry (Fig. 4).[37] The axial bond lengths in the vanadate complex of 2.27 Å and 2.09 Å correspond to axial bond numbers of 0.16 and 0.32 bonds to vanadium from the entering H_2O and leaving ADP, respectively. Assuming the same axial bond lengths to phosphorus in a trigonal bipyramidal transition state yields axial bond numbers of 0.13 and 0.25 bonds to phosphorus from the entering and leaving groups, respectively. Because a fully associative mechanism has an axial bond number of 1.0 to the entering group and a fully dissociative mechanism has no axial bonding in the transition state, these distances suggest a mechanism for myosin ATPase that is 13% associative.

In the F1 ATPase structure (Fig. 5), the oxygen of the attacking water is at hydrogen bonding distances (2.76 and 2.97 Å) from the two carboxylate oxygens of Glu-188, a residue that is therefore well positioned to function as a general base. Glu-188 contributes between $10^{2.8}$- and $10^{4.1}$-fold to multisite ATP hydrolysis as determined by mutating this residue to Gln or Ala.[35,36] The cationic residues Lys-162, Arg-189, and Arg-373 (from the adjacent α-subunit) all interact with the nonbridging oxygens of the γ-phosphoryl group of ATP, at distances of 2.72, 3.04, and 3.10 Å, respectively. Mutations of Lys-162 and Arg-189 result in $10^{3.7}$- to $10^{4.0}$- and $10^{3.8}$-fold decreases in k_{cat}, respectively. A similar $10^{3.7}$-fold decrease in k_{cat} is observed on mutating Thr-163 to Ala. This residue helps to position the γ-phosphoryl group. These activity losses already multiply to 10^{14}–$10^{15.6}$ without even counting the catalytic effects of Arg-373, or of the essential Mg^{2+}, which is β,γ coordinated to ATP and which, in other systems, contributes a factor of $\geq 10^5$ to catalysis (see above). Clearly, the catalytic effects of these residues

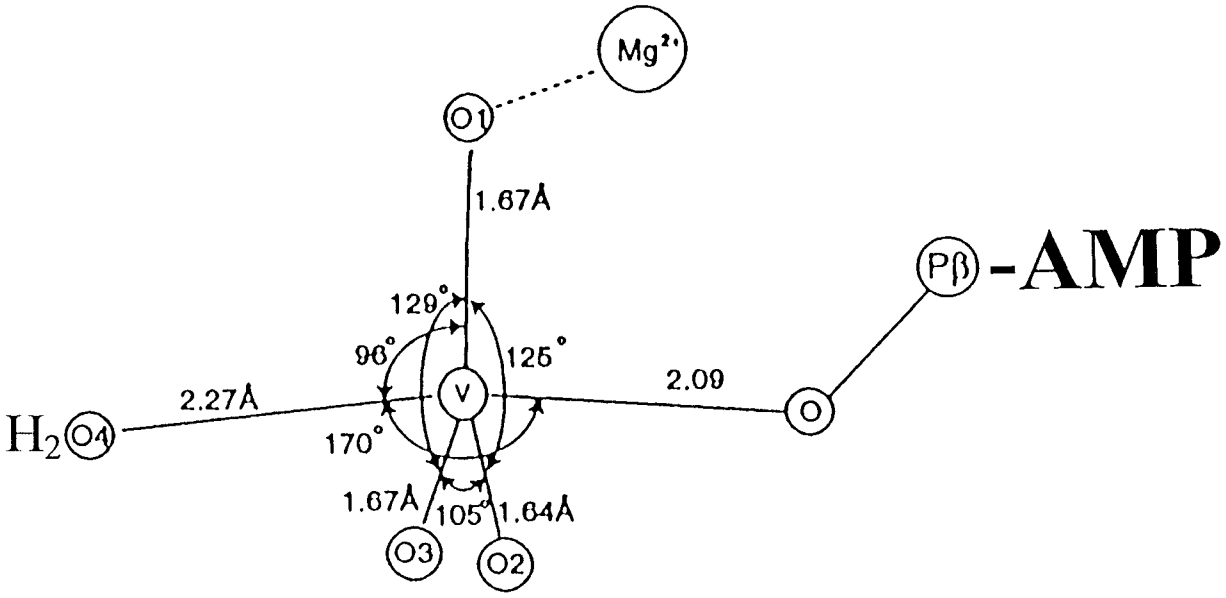

Fig. 4. Myosin ATPase. Geometry and dimensions of vanadate in the enzyme-Mg^{2+}-ADP-VO_4 complex, which mimics the transition state (modified from Ref. 37.)

on $\Delta G^{\neq}$ cannot be additive. They must be partially additive, indicating that they act cooperatively such that the mutation of one residue abolishes not only its own effect but also its cooperative effect with other residues.[38] Because most of the catalytic residues of F1 ATPase interact simultaneously with the γ-phosphoryl group of ATP or with the nearby attacking water, such cooperativity is not surprising. To dissect this cooperativity further would require a study of the kinetic effects of double mutants involving pairs of catalytic residues.

Despite the complexity of F1 ATPase as a model, the X-ray structures of the G proteins,[39] including those of Giα1[40] and transducin,[41,42] readily provide an explanation of their much lower catalytic powers (Table I), which are $10^{3.2}$- and $10^{3.6}$-fold lower than that of F1 ATPase. The reaction coordinate distance to a nearby water is 3.9 Å on both G proteins, values that are probably indistinguishable from the distance of 4.04 Å found on F1 ATPase, indicating a very similar mechanism with some associative character. Consistent with a mechanism for G proteins with some associative character, high-resolution, transition-state structures of Giα1 and transducin of the form E-GDP-O-AlF_4^{2-}-OH_2 have been obtained.[40,42] These complexes form a square bipyramid, similar to, but not isosteric with the trigonal bipyramidal phosphorane transition-state E-GDP-O-PO_3^{2-}-OH_2, which would form in a mechanism with some associative character. The axial Al-O bond lengths of 1.9–2.1 Å are only slightly longer than the axial bond lengths of 1.51–1.79 Å found in stable phosphoranes.[43] Noting that Al, like P, is a third row element, and assuming a trigonal bipyramidal transition state with axial bond lengths equal to those found in the E-GDP-O-AlF_4^{2-}-OH_2 complexes, axial bond numbers to the entering water calculated with Eq. (1) are 0.52 for Giα1 and 0.36 for transducin. These values suggest that the mechanisms of these G proteins are 36–52% associative, approaching an S_N2 mechanism. The axial bond numbers to the leaving GDP on both enzymes are 0.24, suggesting that this bond is 76% broken in the transition state.

A recent proposal of the universality of dissociative mechanisms on G proteins[44] assumes that their mechanisms must be identical to those of dissociative model reactions, which are 10^7-fold slower, and fails to explain the large number of cationic residues on G proteins that interact with the γ-phosphoryl group of GTP (see below). Such interactions would inhibit a dissociative mechanism and promote an associative mechanism.[3] Appropriate model reactions for G proteins can best be chosen when the mechanisms of the G proteins themselves are better understood.

The β,γ coordination of Mg^{2+} found in F1 ATPase and all of the catalytic residues near the γ-phosphoryl group of the bound nucleotide are preserved in G proteins. However, the residue corresponding to Glu-188, the general base, has been replaced by Gln on G proteins. With a pK_a of ~25, Gln cannot ionize to yield a base, contrary to a recent proposal,[42] nor can it readily accept a proton. Indeed, the E188Q mutation of F1 ATPase results in an enzyme with a reduced catalytic power of $10^{7.3\pm0.6}$, indistinguishable from those of Giα1 and transducin.[35,36] Conversely, mutation of this Gln residue to Glu on the G protein, $p21^{ras}$ results in a 20-fold activation of GTP

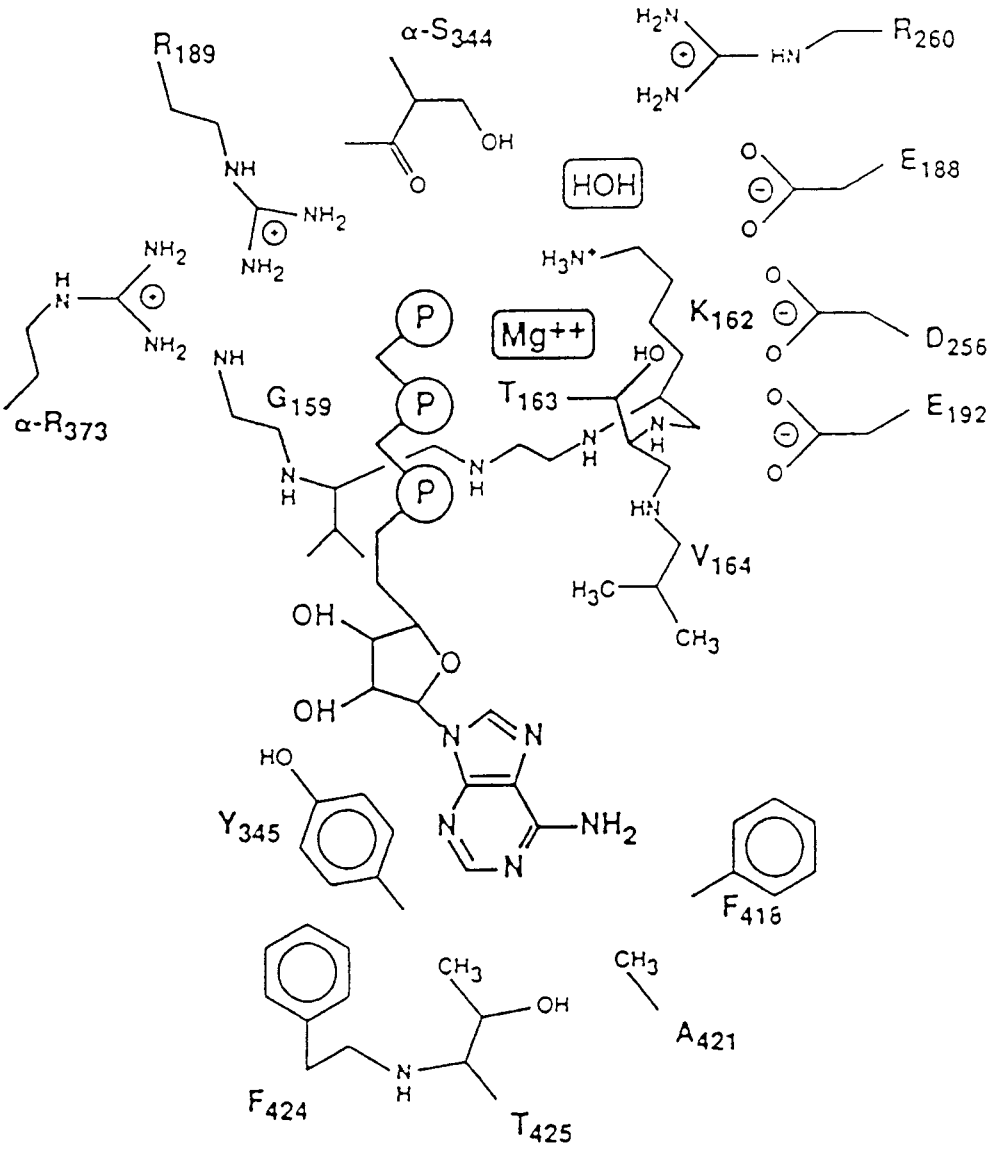

Fig. 5. Bovine mitochondrial F1 ATPase, β-subunit. Active site showing divalent cation activator and residues that are near the bound ADPNP and the bound water.[32]

hydrolysis.[45] Although it cannot function as a general base, Gln-204 of Giα1 (corresponding to Glu-188 of F1 ATPase) does contribute to catalysis by positioning the attacking water near the γ-phosphoryl group of GTP in the transition state (Fig. 6B). Thus, the Q204L mutant of Giα1, although very similar in structure to the wild-type enzyme, shows a $10^{1.8}$-fold lower rate of phosphoryl transfer.[46] Contraction of the transition states of Giα1[40] (and of transducin[42]) are suggested by the observations that Gln-204 (200) moves toward the attacking water and the γ-phosphoryl group of GTP, and Arg-178 (174) moves to interact with fluorines of AlF_4, corresponding to nonbridging oxygens of the transition state, as well as the leaving oxygen of GDP.

In the X-ray structure of the nonactivated αβγ-heterotrimer of transducin, Gln-200 (corresponding to Gln-204 of Giα1), together with the backbone NH of the preceding conserved Gly-199, interact directly with the β-subunit.[47] When activated by GTP binding, Gln-200 moves to orient the attacking water, and Gly-199 moves to donate a hydrogen bond to the γ-phosphoryl group. The loss of these interactions with the β-subunit on GTP binding, as well as nearby conformational changes in the secondary structure of the catalytic α-subunit result in the dissociation of the βγ-dimer from the α-subunit.[47]

The wild-type $p21^{ras}$ enzyme, the slowest of the G proteins, with a catalytic power of only $10^{5.7}$, lacks not only a general base but also a residue correspond-

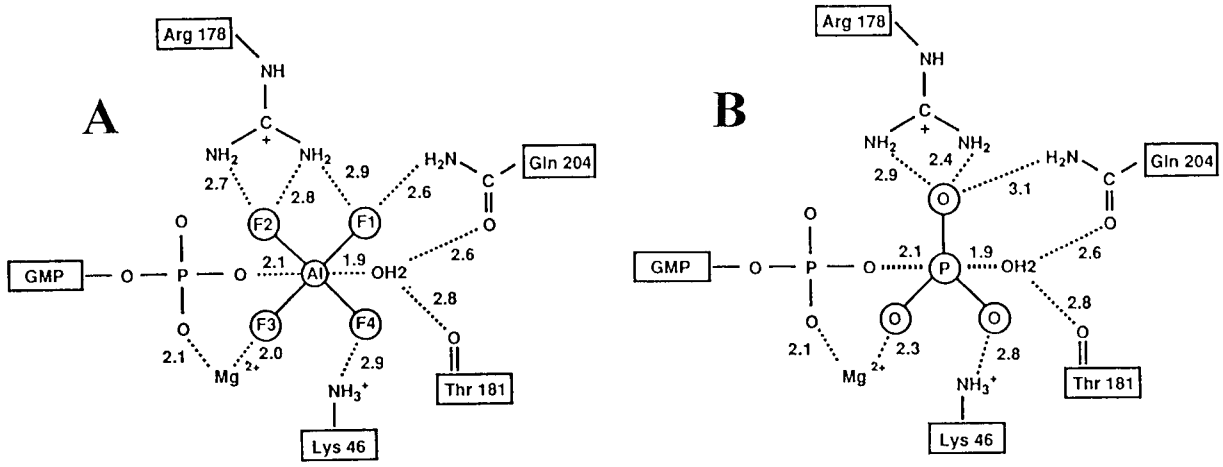

Fig. 6. G-protein Giα1. **A:** Diagram showing the dimensions of the enzyme-GDP-AlF_4-OH_2 complex and nearby residues. **B:** Proposed transition state based on (A).[40]

ing to Arg-189 of F1 ATPase or to Arg-178 of Giα1. This Arg residue interacts with the γ-phosphoryl group and on F1 ATPase contributes a factor of $10^{3.8}$ to ATP hydrolysis. Its homolog on Giα1, Arg-178, contributes a factor of $10^{2.4}$ to GTP hydrolysis.[46] The lack of this residue on $p21^{ras}$ can explain readily its $10^{1.8}$-fold lower catalytic power than that of Giα1. The lack of residues corresponding to both Glu-188 and Arg-189 can explain the 10^5-fold lower activity of $p21^{ras}$ below that of F1 ATPase.

It may therefore be concluded that the slow hydrolysis of GTP on G proteins, which prolongs their active or "switched on" states, is achieved by avoiding the use of general base catalysis. In some cases, further loss of activity is achieved by the lack of other catalytic residues, such as Arg-178, which neutralizes charge and polarizes the γ-phosphoryl group. The resulting enzymes, although damaged as catalysts, function appropriately as switches, properly controlling a variety of biological processes.

The GTPase activities of G proteins can be increased by factors ranging from $10^{1.4}$ to 10^5 by the binding of G-activator (GAP) proteins to the catalytic α-subunit.[48–50] These activator proteins function by further stabilizing the transition state as indicated by parallel increases in the rate of GTP hydrolysis and in the affinity of G proteins for the transition-state analog GDP-O-AlF_4^{2-}-OH_2.[49,50] They may do so by decreasing the distances between catalytic residues and the reaction center, thus further contracting the transition state. In addition, in the case of $p21^{ras}$, the G-activator proteins p120 GAP and neurofibrin, which activate GTP hydrolysis by a factor of 10^5, may also contribute the missing Arg residue, as indicated by the effects of mutation of Arg residues in these proteins.[50,51]

A linear free-energy relationship between the pK_a of the γ-phosphoryl group of enzyme-bound GTP and log (k_{cat}) on several mutants of $p21^{ras}$ with a slope of 2.1 has been rationalized by assuming a prior proton transfer from the attacking water to the γ-phosphoryl group, followed by a rate-limiting nucleophilic attack by OH^- on the γ-phosphorus.[52,53] In this highly associative mechanism, the γ-phosphoryl group of MgGTP itself is proposed to function as a general base. However, by invoking general base catalysis, this mechanism fails to explain why $p21^{ras}$ and other G proteins are poorer catalysts than F1 ATPase, which has a nearby glutamate residue. Because only a small and inverse D_2O solvent isotope effect on k_{cat} was observed,[53] proton transfer may not be involved at all. An alternative explanation for the strong correlation of hydrolysis rate with basicity of the γ-phosphoryl group is progressively stronger, cooperative interactions of the multiple cationic catalytic residues of the enzyme with the γ-phosphoryl group as its basicity is increased, thus further stabilizing the transition state. This alternative explanation is supported by the authors' own observation that $p21^{ras}$, when activated by neurofibrin, a GAP-like activator protein that may provide an additional Arg residue to interact with the γ-phosphoryl group, shows a stronger linear free-energy relationship with a slope of 4.9.[52]

PHOSPHOSERINE-PHOSPHOTHREONINE PROTEIN PHOSPHATASES

This subject recently was reviewed from a structural perspective.[54] Like *E. coli* alkaline phosphatase, which has a binuclear Zn^{2+} center at its active site, those of P-Ser/P-Thr protein phosphatases also have binuclear metal centers with two transition metals (Zn^{2+}-O-Fe^{2+} in PP2B and Mn^{2+}-O-Fe^{2+} in PP1). However, unlike alkaline phosphatase, which functions via a covalent phosphoenzyme (phosphoserine) intermediate that is attacked by water in a

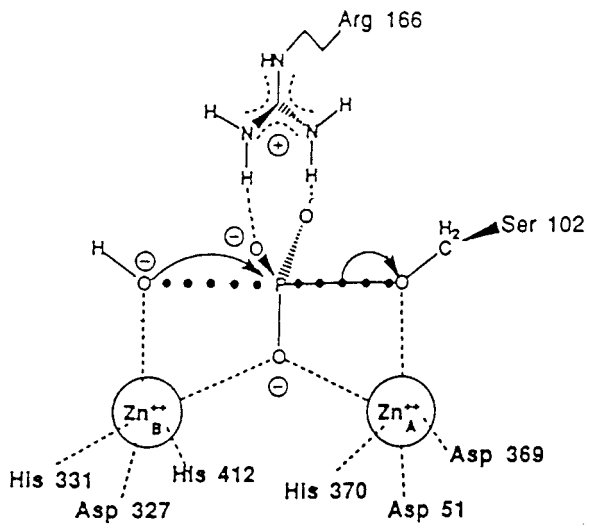

Fig. 7. *E. coli* alkaline phosphatase. Proposed transition state of the second step in which phosphoserine-102 is hydrolyzed, based on the X-ray structure[56] and on the kinetic effects of mutations[62,63] (modified from Ref. 57).

second step, P-Ser/P-Thr protein phosphatases show no kinetic evidence of a covalent phosphoenzyme intermediate, and a mechanistically related enzyme shows stereochemical inversion at phosphorus, indicating a single substitution.[55] Hence, the reactions catalyzed by P-Ser/P-Thr phosphatases are analogous to the second half of the alkaline phosphatase reaction, but in which an *exogenous* P-Ser of the protein substrate is attacked by water.

With alkaline phosphatase, which may serve as a structural model for P-Ser/P-Thr protein phosphatases, the reasonable mechanistic assumption has been made that in the transition state, the leaving oxygen is coordinated by one Zn^{2+} and the entering oxygen is coordinated by the other Zn^{2+} of the binuclear center (Fig. 7).[6,56,57,58] The distance of 3.94 Å between the two Zn^{2+} ions then would approximate closely the distance between the entering and leaving oxygens in the trigonal bipyramidal transition state.[56] If the transition state is symmetric, the axial bond length to the entering group (1.97 Å) corresponds to an axial bond number of 0.40, indicating a mechanism for alkaline phosphatase which is 40% associative, approaching an S_N2 mechanism. An asymmetric transition state would increase the associative character of the mechanism.

A careful measurement by linear free-energy relations with thiophosphate substrates, of the sensitivity of k_{cat}/K_m to the basicity of the leaving group yielded a β-value of -0.77.[6] This β-value was interpreted in terms of a dissociative transition state, based on model reactions in solution, which were reinterpreted to predict a less negative β-value of -0.1 to -0.2 for k_{cat}/K_m in an associative mechanism. However, because the leaving group departs in *both* associative and dissociative mechanisms, the β-leaving group is not diagnostic of mechanism. Indeed, phosphotriesterase, an enzyme that catalyzes a highly associative reaction, shows β-leaving group values ranging from -2.0 to -3.2, depending on the metal ion activator.[59] Moreover, unlike the model reactions, on an enzyme the distance between the entering and leaving atoms can be fixed, in the present case by coordination to the two Zn^{2+} ions. When the axial distance is thus constrained in the transition state, the greater the cleavage of the bond to the leaving group, the greater the formation of the bond to the entering group. Hence, if the bond to the leaving group were 77% broken in the transition state (i.e., 0.23 of a bond) as suggested by the β-leaving group, its length would be 2.11 Å from Eq. (1). The bond to the entering group would be 3.94 Å minus 2.11 Å or 1.83 Å, corresponding to 0.68 of a bond and to a mechanism that is 68% associative. Consistent with a highly associative mechanism, the attacked phosphoryl group is surrounded by cationic centers, two Zn^{2+} ions and Arg-166, which acts as a bifunctional hydrogen bond donor.[56]

The high catalytic power of 10^{11} for alkaline phosphatase may be rationalized by the binuclear Zn^{2+} site, which contributes $\geq 10^{10}$ to catalysis and by Arg-166, which contributes $10^{1.5}$ to transition-state stabilization. Each divalent cation is assumed to contribute a factor of $\geq 10^5$ based on the kinetic effects of metal variation on Staphylococcal nuclease,[1] and of mutating metal ligands on the MutT enzyme[60] and on the λ-P-ser/P-Thr protein phosphatase.[61] The factor of $10^{1.5}$ for Arg-166 is based on the effects on k_{cat} of mutating this residue to an uncharged amino acid.[62,63] No kinetic or structural evidence for general base catalysis has been provided, and none is required to explain the catalytic power of alkaline phosphatase. Because of its high pH optimum, specific base catalysis by OH^- may occur.

Although similar active sites for P-Ser/P-Thr protein phosphatases suggest a similar associative mechanism, the orientation of the substrate, based on the position of the tetrahedral tungstate anion coordinated by both Mn^{2+} and Fe^{2+} on PP1, and of a phosphate bound in the second coordination sphere of both Mn^{2+} sites in PP2c is not precisely determined.[54,64] Two conserved Arg residues, 96 and 221, interact monofunctionally with tungstate oxygens on PP1, (Fig. 8), and one Arg interacts bifunctionally with phosphate on PP2c. As on alkaline phosphatase, metal-bound water ligands are positioned to attack the substrate, and no structural or kinetic evidence for general base catalysis has been reported. However, the leaving oxygen is not directly coordinated to a metal ion. Instead, on PP1, His-125 is positioned to act as a general acid catalyst to protonate the leaving oxygen (Fig. 8).

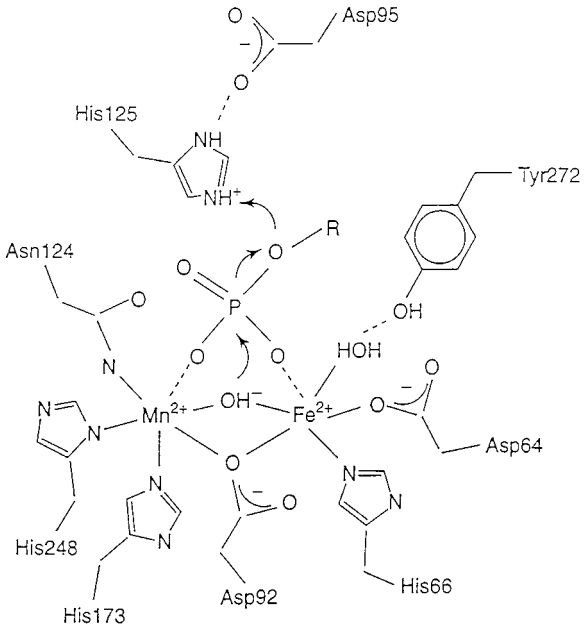

Fig. 8. P-Ser/P-Thr protein phosphatase. Mechanism based on the X-ray structure[64] and on kinetic studies of mutants.[61]

From the effects of single mutations on k_{cat} of the homologous λ-PPase,[61] transition-state stabilization by Arg-96 could contribute a factor of $10^{3.5}$ to catalysis, general acid catalysis by His-125 a factor of $10^{5.0}$, and metal ion catalysis by one of the two metals of the binuclear cluster could contribute $\geq 10^5$, because the second metal does not appear to participate directly by coordinating the leaving oxygen. Assuming additivity of these effects on $\Delta G^{\neq}$, a combined factor of $\geq 10^{13.5}$ is obtained, which slightly exceeds the catalytic power of λ-PPpase ($10^{12.7}$) even without consideration of a more direct role of the second metal ion, or of Arg-221, which has not been mutated. Hence, like F1 ATPase, the metal ion(s) and catalytic residues are likely acting cooperatively, which would make their catalytic effects on $\Delta G^{\neq}$ partially additive rather than additive. This point has not been tested by studies of double mutants.

PHOSPHOTYROSINE PROTEIN PHOSPHATASES

Unlike P-Ser/P-Thr protein phosphatases, P-Tyr protein phosphatases use no metal cations and proceed through a kinetically competent, covalent phosphocysteine intermediate which, in a second step, is hydrolyzed by water.[65,66] On the basis of their X-ray structures, the active sites of four P-Tyr phosphatases are very similar.[67–70] An extensively studied member of this class is the bacterial enzyme from Yersinia,[67] and a mechanism is shown in Figure 9. A model of the transition states for both steps, based on the X-ray structure of the vanadate complex, E-S-VO_3-OH, shows a trigonal bipyramid with an axial V-S bond length of 2.52 Å and an axial V-O bond length of 1.94 Å.[71]¶ Assuming the same axial bond lengths in the "phosphorane" transition state and single bond P-S and P-O distances of 2.12 and 1.73 Å, respectively, one obtains from Eq. 1 axial bond numbers of 0.21 for P—S and 0.45 for P—O in the transition states. These bond numbers indicate a mechanism that is 21% associative (or 79% dissociative) in the first step and 45% associative (or 55% dissociative) in the second step. These estimates are consistent with the differing nucleophilicites of the entering groups in the two steps, if the second nucleophile were OH^-. Sizable primary ^{18}O kinetic isotope effects, which are consistent with significant bond breakage to the *leaving* tyrosine in the transition state of the first step, have been interpreted in terms of a highly dissociative mechanism.[72] However, these effects provide no information on the extent of *entry* by the cysteine thiolate, which is much more diagnostic of mechanism. An inverse secondary ^{18}O effect of the nonbridge oxygens, expected in a highly dissociative mechanism, was not found, requiring the assumption of a dianionic resonance form of metaphosphate. Although theoretically possible,[73,74] such a species would be expected to contribute more when there is nucleophilic participation by the thiolate. In mutants lacking the general acid catalyst, Asp-356, a normal secondary, nonbridge ^{18}O isotope effect was detected, reflecting an increase in the associative character of the mechanism. However, the isotope effects were smaller than expected for a highly associative process.[4] Alcoholysis of the E-P intermediate of the yeast enzyme yielded a β-nucleophilicity of 0.14,[74a] suggesting a mechanism which is only 14% associative.

The high catalytic power of the Yersinia P-Tyr protein phosphatase of 10^{11} can be explained on the basis of the X-ray structure of the tungstate complex[67] and mutational studies,[75] taking into account that, under certain conditions, the formation of the thiophosphoryl intermediate is the rate-limiting step. The nucleophilic cysteine residue at the active site, Cys-403, is part of an anion binding loop with the consensus sequence, -HCXAGXXR-. The pK_a value of Cys-403 is 4.7, which is 3.8 units lower than the value of 8.5 expected for an exposed Cys residue in an unstructured environment.[76] This low pK_a, which eliminates the need for a general base and thereby contributes $10^{3.8}$ to catalysis, is due to the summation of α-helix dipole effects,[67] the proximity of Arg-409,[69] and the polarization of the backbone carbonyl of Cys-403 by His-402.[76] Asp-356, which serves as the acid catalyst to protonate the leaving tyrosinate, contributes a factor of 10^3, based on the effect of its mutation.[75] Arg-404, which is hydrogen

¶J. Vijayalakshmi, M.A. Saper, and J. Dixon, personal communication, 1997.

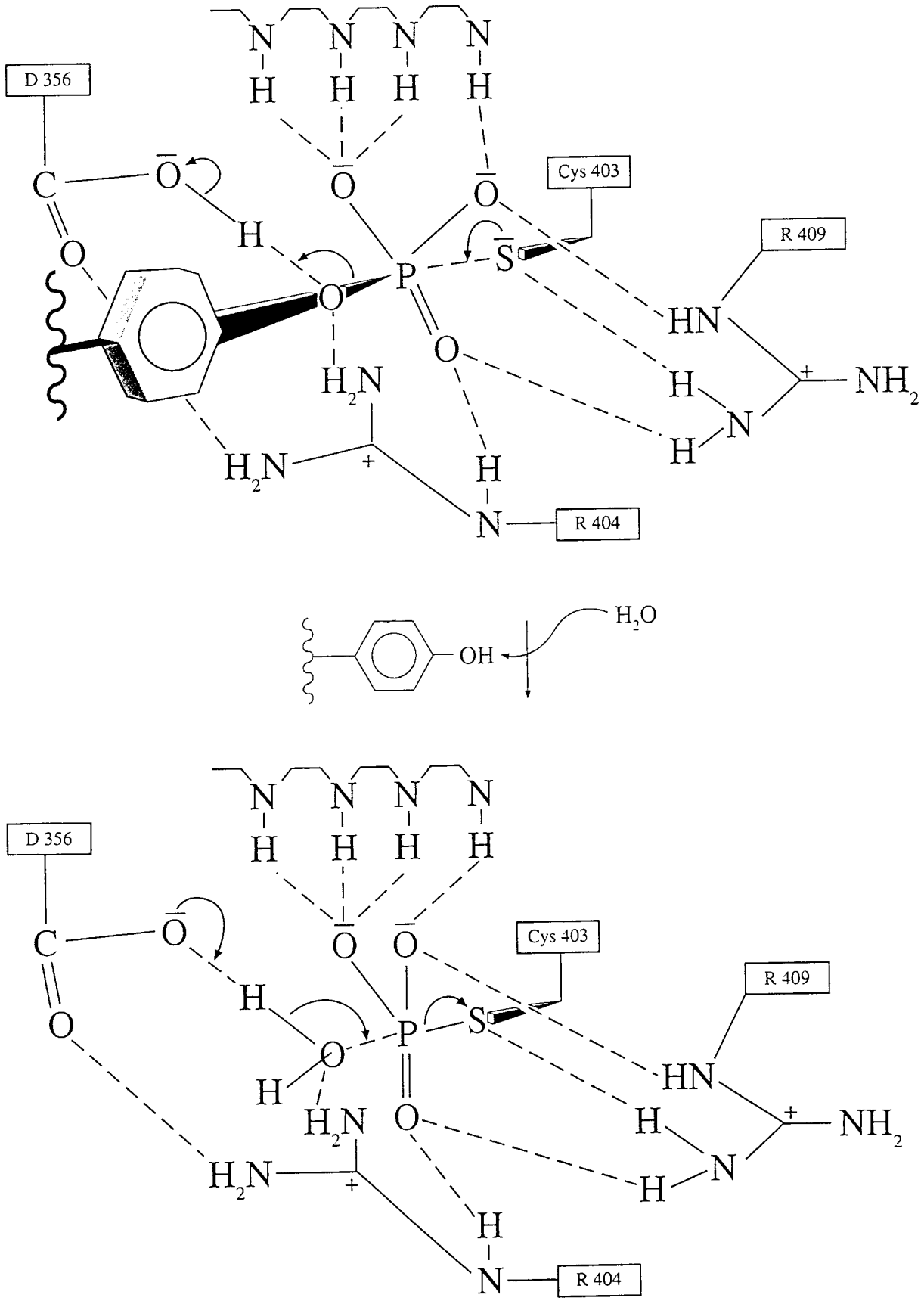

Fig. 9. P-Tyr protein phosphatase. Mechanism based on the X-ray structure[67] and on kinetic studies of the wild type[65,66] and mutant enzymes.[75] In the second half of the reaction (bottom), a serine residue may also participate in catalysis on some P-Tyr protein phosphatases.[74a,90,91]

bonded to a nonbridge oxygen and to the leaving oxygen of phosphotyrosine (and to Asp-356), contributes at least 10^2. Arg-409, which is oriented by Glu-290 to interact with two nonbridging oxygens of phosphotyrosine, contributes 10^2, as inferred from the effects of mutating Glu-290.[75] Assuming additivity of these effects on $\Delta G^{\neq}$, which has not been tested by double mutants, a catalytic power $\geq 10^{10.8}$ is estimated, which closely approaches the observed value of 10^{11}-fold (Table I).

The dual-specificity protein phosphatases, which catalyze not only P-Tyr hydrolysis but also the much slower hydrolysis of P-Ser and P-Thr residues, show tertiary structures (but not primary structures) which closely resemble those of the P-Tyr protein phosphatases.[70] Their mechanisms appear to be very similar,[76] but the active sites of the dual-specificity enzymes are shallower, permitting entry of the shorter P-Ser and P-Thr residues.

ACKNOWLEDGMENTS

I thank Philip A. Cole, T.K. Harris, W.W. Cleland, Susan S. Taylor, Ron A. Kohanski, Mario Bianchet, Jack Dixon, John Sondek, Young Hee Ko, Peter L. Pedersen, and George Sack for valuable discussions.

REFERENCES

1. Serpersu, E.H., Shortle, D., Mildvan, A.S. Kinetic and magnetic resonance studies of active site mutants of staphylococcal nuclease: Factors contributing to catalysis. Biochemistry 26:1289–1300, 1987.
2. Radzicka, A., Wolfenden, R. A proficient enzyme. Science 267:90–93, 1995.
3. Mildvan, A.S., Fry, D.C. NMR studies of mechanism of enzyme action. Adv. Enzymol. Relat. Areas Mol. Biol. 59:241–313, 1987.
4. Cleland, W.W., Hengge, A.C. Mechanisms of phosphoryl and acyl transfer. FASEB J. 9:1585–1594, 1995.
5. Pauling, L. "The Nature of the Chemical Bond." 3rd ed. Ithaca, NY: Cornell University Press, 255–260, 1960.
6. Hollfelder, F., Herschlag, D. The nature of the transition state for enzyme-catalyzed phosphoryl transfer: Hydrolysis of O-aryl phosphorothioates by alkaline phosphatase. Biochemistry 34:12255–12264, 1995.
7. Mildvan, A.S. Conformations and arrangements of substrates at active sites of ATP-utilizing enzymes. Philos. Trans. R. Soc. [Biol.] 293:65–74, 1981.
8. Weber, D.J., Gittis, A.G., Mullen, G.P., Abeygunawardana, C., Lattman, E.E., Mildvan, A.S. NMR docking of a substrate into the x-ray structure of staphylococcal nuclease. Proteins 13:275–287, 1992.
9. Weber, D.J., Serpersu, E.H., Gittis, A.G., Lattman, E.E., Mildvan, A.S. NMR docking of the competitive inhibitor 3′,5′-pdTp into the x-ray structure of staphylococcal nuclease. Proteins 17:20–35, 1993.
10. Serpersu, E.H., McCracken, J., Peisach, J., Mildvan, A.S. Electron spin echo modulation and nuclear relaxation studies of staphylococcal nuclease and its metal-coordinating mutants. Biochemistry 27:8034–8044, 1988.
11. Pourmotabbed, T., Dell'Acqua, M., Gerlt, J.A., Stanczyk, S., Bolton, P.H. Kinetic and conformational effects of lysine substitutions for arginines 35 and 87 in the active site of staphylococcal nuclease. Biochemistry 29:3677–3683, 1990.
12. Mildvan, A.S. Qualitative and quantitative aspects of the mechanisms of DNA and RNA nucleases. FASEB J. 6:A266, 1992.
13. Stivers, J.T., Shuman, S., Mildvan, A.S. Vaccinia DNA topoisomerase I: Single turnover and steady state analysis of DNA strand cleavage and ligation reactions. Biochemistry 33:327–339, 1994.
14. Hunter, T., Plowman, G.D. The protein kinases of budding yeast: Six score and more. Trends Biochem. Sci. 22:18–22, 1997.
15. Walsh, P.A., Krebs, E.G. Protein kinases. "The Enzymes." Boyer, P.D. (ed.). New York: Academic Press, 8:555–581, 1973.
16. Beebe, S.J., Corbin, J.D. Cyclic nucleotide dependent protein kinases. "The Enzymes." Boyer, P.D., Krebs, E.G. (eds.). New York: Academic Press, 17:43–111, 1986.
17. Mildvan, A.S. "Enzymes Utilizing ATP: Kinases, ATPases, and Polymerases. Encyclopedia of NMR. Chichester, UK: Wiley & Sons Ltd., 1909–1918, 1996.
18. Madhusudan, Trafny, E.A., Xuong, N.-H., Adams, J.A., Ten Eyck, L.F., Taylor S.S., Sowadski, J.M. cAMP protein kinase: Crystallographic insights into substrate recognition and phosphotransfer. Protein Sci. 3:176–187, 1994.
19. Bossmeyer, D., Engh, R.A., Kinzel, V., Ponstingl, H., Huber, R. Phosphotransferase and substrate binding mechanism of the cAMP-dependent protein kinase catalytic subunit from porcine heart as deduced from the 2.0 Å structure of the complex with Mn2+ adenylyl imidodiphosphate and inhibitor peptide PKI(5-24). EMBO J. 12:849–859, 1993.
20. Granot J., Kondo, H., Armstrong, R.N., Mildvan, A.S., Kaiser, E.T. NMR studies of the conformation of tetraaminecobalt(III)ATP bound at the active site of bovine heart protein kinase. Biochemistry 18:2339–2345, 1979.
21. Granot, J., Mildvan, A.S., Brown, E.M., Kondo, H., Bramson, H.N., Kaiser, E.T. Specificity of bovine heart protein kinase for the Δ-stereoisomer of the metal-ATP complex. FEBS Lett. 103:265–269, 1979.
22. Rosevear, P.R., Fry, D.C., Mildvan, A.S., Doughty, M., O'Brian, C., Kaiser, E.T. NMR studies of the backbone protons and secondary structure of pentapeptide and heptapeptide substrates bound to bovine heart protein kinase. Biochemistry 23:3161–3173, 1984.
23. Bramson, H.N., Thomas, N.E., Miller, W.T., Fry, D.C., Mildvan, A.S., Kaiser, E.T. Conformation of Leu-Arg-Arg-Ala-Ser-Leu-Gly bound in the active site of 3′,5′ cAMP-dependent protein kinase. Biochemistry 26:4466–4470, 1987.
24. Knighton, D.R., Zheng, J., Ten Eyck, L.F., Xuong, N.-H., Taylor, S.S., Sowadski, J.M. Structure of a peptide inhibitor bound to the catalytic subunit of cAMP-dependent protein kinase. Science 253:414–420, 1991.
25. Rosevear, P.R., Bramson, H.N., O'Brian, C., Kaiser, E.T., Mildvan, A.S. NOE studies of the conformation of tetraaminecobalt(III)ATP free and bound to the bovine heart protein kinase. Biochemistry 22:3439–3447, 1983.
26. Granot, J., Mildvan, A.S., Bramson, H.N., Kaiser, E.T. Magnetic resonance measurements of intersubstrate distances at the active site of protein kinase using substitution insert Co(III) and Cr(III) complexes of adenosine 5′-(β,γ-methylene triphosphate). Biochemistry 19:3537–3543, 1980.
27. Grant, B.D., Adams, J.A. Presteady state kinetic analysis of cAMP-dependent protein kinase using rapid quench flow techniques. Biochemistry 35:2022–2029, 1996.
28. Gibbs, C.S., Zoller, M.J. Rational scanning mutagenesis of a protein kinase identifies functional regions involved in catalysis and substrate interactions. J. Biol. Chem. 266: 8923–8931, 1991.
29. Hubbard, S.R., Wei, L., Ellis, L., Hendrickson, W.A. Crystal structure of the tyrosine kinase domain of the human insulin receptor. Nature 372:746–754, 1994.
30. Grace, M.R., Walsh, C.T., Cole, P.A. Divalent ion effects and insights into the catalytic mechanism of protein tyrosine kinase Csk. Biochemistry 36:1874–1881, 1997.

30a. Kim, K. Cole, P.A. Measurement of a Bronsted nucleophile coefficent and insights into the transition state for a protein tyrosine kinase. J Am. Chem. Soc. 119 (in press), 1997.

31. Kemp, B.E., Graves, D.J., Benjamini, E., Krebs, E.G. Role of multiple basic residues in determining the substrate

specificity of cAMP-dependent protein kinase. J. Biol. Chem. 252:4888–4894, 1977.
32. Abrahams, J.P., Leslie, A.G.W., Lutter, R., Walker, J.E. Structure at 2.8 Å resolution of F1-ATPase from bovine heart mitochondria. Nature 370:621–628, 1994.
33. Bianchet, M.A., Hullihen, J., Pedersen, P.L., Amzel, L.M. Three dimensional structure of the active form of mitochondrial ATPase: ATP hydrolysis/synthesis involves subtle conformational changes (submitted for publication).
34. Omote, H., Maeda, M., Futai, M. Effects of mutations of conserved Lys-155 and Thr-156 residues in the phosphate binding glycine-rich sequence of the F1-ATPase β subunit of E. coli. J. Biol. Chem. 267:20571–20576, 1992.
35. Senior, A.E., Al-Shawi, M.K. Further examination of seventeen mutations in E. coli F1-ATPase β-subunit. J. Biol. Chem. 267:21471–21478, 1992.
36. Park, M.-Y., Omote, H., Maeda, M., Futai, M. Conserved Glu-181 and Arg-182 residues of E. coli H^+-ATPase (ATP synthase) β subunit are essential for catalysis: Properties of 33 mutants between βGlu-161 and βLys-201 residues. J. Biochem. 116:1139–1145, 1994.
37. Smith, C.A., Rayment, I. X-ray structure of the Mg(II)·ADP·Vanadate complex of the Dictyostelium discoideum myosin motor domain to 1.9 Å resolution. Biochemistry 35:5404–5417, 1996.
38. Mildvan, A.S., Weber, D.J., Kuliopulos, A. Quantitative interpretations of double mutations of enzymes. Arch Biochem. Biophys. 294:327–340, 1992.
39. Kjeldgaard, M., Nyborg, J., Clark, B.F.C. The GTP binding motif: Variations on a theme. FASEB J. 10:1347–1368, 1996.
40. Coleman, D.E., Berghius, A.M., Lee, E., Linder, M.E., Gilman, A.E., Sprang, S.R. Structures of active conformations of $G_{i\alpha 1}$ and the mechanism of GTP hydrolysis. Science 265:1405–1412, 1994.
41. Noel, J.P., Hamm, H.E., Sigler, P.B. The 2.2 Å crystal structure of transducin α complexed with GTPγS. Nature 366:654–663, 1993.
42. Sondek, J., Lambright, D.G., Noel, J.P., Hamm, H.E., Sigler, P.B. GTPase mechanism of G proteins from the 1.7 Å crystal structure of transducin α·GDP·$A1F_4$. Nature 372: 276–279, 1994.
43. Ramirez, F., Ugi, I. Turnstile rearrangement and pseudorotation in the permutational isomerization of pentavalent phosphorous compounds. Adv. Phys. Org. Chem. 9:25–126, 1971.
44. Maegly, K.A., Admiraal, S.J., Herschlag, D. Ras-catalysed hydrolysis of GTP: A new perspective from model studies. Proc. Natl. Acad. Sci. USA 93:8160–8166, 1996.
45. Frech, M., Darden, T.A., Pedersen, L.G., Foley, C.K., Charifson, P.S., Anderson, M.W., Wittinghofer, A. Role of Glu-61 in the hydrolysis of GTP by $P21^{Hras}$ an experimental and theoretical study. Biochemistry 33:3237–3244, 1994.
46. Kleuss, C., Raw, A.S., Lee, E., Sprang, S.R., Gilman, A.G. Mechanism of GTP hydrolysis by G protein α subunits. Proc. Natl. Acad. Sci. USA 91:9828–9831, 1994.
47. Lambright, D.G., Sondek, J., Bohm, A., Skiba, N.P., Hamm, H.E., Sigler, P.B. The 2.0 Å crystal structure of a heterotrimeric G protein. Nature 379:311–319, 1996.
48. Eccleston, J.F., Moore, K.J.M., Morgan, L., Skinner, R.H., Lowe, P.N. Kinetics of interaction between normal and Pro-12 Ras and the GTPase activating proteins P120-GAP and neurofibrin. J. Biol. Chem. 268:27012–27019, 1993.
49. Berman, D.M., Kozasa, T., Gilman, A.G. The GTPase-activating protein RG54 stabilizes the transition state for nucleotide hydrolysis. J. Biol. Chem. 271:27209–27212, 1996.
50. Mittal, R., Zhamadian, M.R., Goody, R.S., Wittinghoffer, A. Formation of a transition state analog of the Ras GTPase reaction by Ras·GDP, tetrafluoraluminate, and GTPase-activating proteins. Science 273:115–117, 1996.
51. Skinner, R.H., Bradley, S., Brown, A.L., Johnson, N.J.E., Rhodes, S., Stammers, D.K., Lowe, P.N. Use of the glu-glu-phe C-terminal epitope for rapid purification of the catalytic domain of normal and mutant ras GTPase-activating proteins. J. Biol. Chem. 266:14163–14166, 1991.
52. Schweins, T., Geyer, M., Kalbitzer, H.R., Wittinghoffer, A., Warshel, A. Linear free energy relationships in the intrinsic and GTP activating protein stimulated GTP hydrolysis of $P21^{ras}$. Biochemistry 35:14225–14231, 1996.
53. Schweins, T., Warshel, A. Mechanistic analysis of the observed linear free energy relationships in $P21^{ras}$ and related systems. Biochemistry 35:14232–14243, 1996.
54. Barford, D. Molecular mechanisms of the protein serine/threosine/phosphatases. Trends Biochem. Sci. 21:407–412, 1996.
55. Mueller, E.G., Crowder, M.W., Averill, B.A., Knowles, J.R. Purple acid phosphatase: A diiron enzyme that catalyzes a direct phospho group transfer to water. J. Am. Chem. Soc. 115:2974–2975, 1993.
56. Kim, E.E., Wyckoff, H.W. Reaction mechanism of alkaline phosphatase based on crystal structures: Two metal ion catalysis. J. Mol. Biol. 218:449–464, 1991.
57. Steitz, T.A., Steitz, J.A. A general two-metal-ion mechanism for catalytic RNA. Proc. Natl. Acad. Sci. USA 90:6498–6502, 1993.
58. Sträter, N., Lipscomb, W.N., Klabunde, T., Krebs, B. Two-metal ion catalysis in enzymatic acyl- and phosphoryl transfer reactions. Angew. Chem. Int. Ed. Engl. 35:2024–2055, 1996.
59. Hong, S.-B., Raushel, F.M. Metal-substrate interactions facilitate the catalytic activity of the bacterial phosphotriesterase. Biochemistry 35:10904–10912, 1996.
60. Lin, J., Abeygunawardana, C., Frick, D.N., Bessman, M.J., Mildvan, A.S. The role of Glu-57 in the mechanism of the E. coli MutT enzyme by mutagenesis and heteronuclear NMR. Biochemistry 35:6715–6726, 1996.
61. Zhuo, S., Clemens, J.C., Stone, R., Dixon, J.E. Mutational analyses of a Ser/Thr phosphatase. J. Biol. Chem. 269: 29234–29238, 1994.
62. Chaidaroglow, A., Brezinski, D.J., Middleton, S.A., Kantrowitz, E.R. Function of Arg-166 in the active site of E. coli alkaline phosphatase. Biochemistry 27:8338–8343, 1988.
63. Butler-Ransohoff, J.E., Kendall, D.A., Kaiser, E.T. Use of site directed mutagenesis to elucidate the role of Arg-166 in the catalytic mechanism of alkaline phosphatase. Proc. Natl. Acad. Sci. USA 85:4276–4278, 1988.
64. Egloff, M.P., Cohen, P.T.W., Reinemer, P., Barford, D. Crystal structure of the catalytic subunit of human protein phosphatase 1 and its complex with tungstate. J. Mol. Biol. 254:942–959, 1995.
65. Cho, H., Ravichandran, K., Kitas, E., Bannwarth, W., Walsh, C.T., Anderson, K.S. Isolation and structural elucidation of a novel phosphocysteine intermediate in the LAR protein tyrosine phosphatase enzymatic pathway. J. Am. Chem. Soc. 114:7296–7298, 1992.
66. Guan, K., Dixon, J.E. Evidence for protein-tyrosine-phosphatase catalysis proceeding via cysteine-phosphate intermediate. J. Biol. Chem. 266:17026–17030, 1991.
67. Stuckey, J.A., Schubert, H.L., Fauman, E.B., Zhang, Z.-Y., Dixon, J.E., Saper, M.A. Crystal structure of Yersinia protein tyrosine phosphatase at 2.5 Å and the complex with tungstate. Nature 370:571–575, 1994.
68. Su, X.-D., Taddei, N., Stefani, M., Ramponi, G., Nordlund, P. The crystal structure of a low molecular weight phosphotyrosine protein phosphatase. Nature 370:575–578, 1994.
69. Barford, D., Flint, A.J., Tonks, N.K. Crystal structure of protein tyrosine phosphatase 1B. Science 263:1397–1404, 1994.
70. Fauman, E.B., Saper, M.A. Structure and function of the protein tyrosine phosphatases. Trends Biochem. Sci. 21: 413–417, 1996.
71. Denu, J.M., Lohse, D.L., Vijayalakshmi, J., Saper, M.A., Dixon, J.E. Visualization of intermediate and transition state structures in protein tyrosine phosphatase catalysis. Proc. Natl. Acad. Sci. USA 93:2493–2498, 1996.
72. Hengge, A.C., Sowa, G.A., Wu, L., Zhang, Z.-Y. Nature of the transition state of the protein tyrosine phosphatase-catalyzed reaction. Biochemistry 34:13982–13987, 1995.
73. Rajca, A., Rice, J.E., Streitweiser, A., Jr., Schaefer, H.F. III. Metaphosphate and tris (methylene) metaphosphate an-

ions. Do they have three double bonds to phosphorus? J. Am. Chem. Soc. 109:4189–4192, 1987.
74. Horn, H., Ahlrichs, R. Energetic measure for the ionic character of bonds. J. Am. Chem. Soc. 112:2121–2124, 1990.
74a. Zhao, Y., Zhan, Z.-Y. Reactivity of alcohols toward the phosphoenzyme intermediate in the protein tyrosine phosphatase-catalyzed reaction: Probing the transition state of the dephosphorylation step. Biochemistry 35:11797–11804, 1996,
75. Zhang, Z.-Y., Wang, Y., Dixon, J.E. Dissecting the catalytic mechanism of protein tyrosine phosphatases. Proc. Natl. Acad. Sci. USA 91:1624–1627, 1994.
76. Denu, J.M., Zhou, G., Guo, Y., Dixon, J.E. The catalytic role of Asp-92 in a human dual-specific protein tyrosine phosphatase. Biochemistry 34:3396–3403, 1995.
77. Zhang, Z.-Y., Dixon, J.E. Active site labeling of the Yersinia protein tyrosine phosphatase: The determination of the pKa of the active site cysteine and the function of the conserved Histidine-402. Biochemistry 32:9340–9345, 1993.
78. Wang, C., Lee, T.R., Lawrence, D.S., Adams, J.A. Rate-determining steps for tyrosine phosphorylation by the kinase domain of v-fps. Biochemistry 35:1533–1539, 1996.
79. Boerner, R.J., Barker, S.C., Knight, W.B. Kinetic mechanism of the foreward and reverse $pp60^{C\text{-}Src}$ tyrosine kinase reaction. Biochemistry 34:16419–16423, 1995.
80. Kohanski, R.A. Insulin receptor autophosphorylation I. Autophosphorylation kinetics of the native receptor and its cytoplasmic kinase domain. Biochemistry 32:5766–5772, 1993.
81. Nakashima, R.A., Paggi, M., Scott, L., Pedersen, P.L. Purification and characterization of a bindable form of mitochondrial bound hexokinase from the highly glycolytic AS-30D rat hepatoma cell line. Cancer Res. 48:913–919, 1988.
82. Linder, M.E., Ewald, D.A., Miller, R.J., Gilman, A.G. Purification and characterization of $G_{o\alpha}$ and three types of $G_{i\alpha}$ after expression in E. coli. J. Biol. Chem. 265:8243–8251, 1990.
83. Arshavsky, V.Y., Dumke, C.L., Zhu, Y., Artemyev, N.O., Skiba, N.P., Hamm, H.E., Bownds, M.D. Regulation of transducin GTPase activity in bovine rod outer segments. J. Biol. Chem. 269:19882–19887, 1994.
84. Trentham, D.R., Eccleston, J.F., Bagshaw, C.R. Kinetic analysis of ATPase mechanisms. Q. Rev. Biophys. 9:217–281, 1976.
85. Hull, W.E., Halford, S.E., Gutfreund, H., Sykes, B.D. 31P NMR study of alkaline phosphatase: The role of inorganic phosphate in limiting the enzyme turnover rate at alkaline pH. Biochemistry 15:1547–1561, 1976.
86. Van Wazer, J.R., Griffith, E.J., McCullogh, J.F. Structure and properties of the condensed phosphates. VII. Hydrolytic degradation of pyro- and tripolyphosphate. J. Am. Chem. Soc. 77:287–291, 1955.
87. Kirby, A.J., Varvoglis, A.G. The reactivity of phosphate esters. Monoester hydrolysis. J. Am. Chem. Soc. 89:415–423, 1967.
88. Bruice, T.C., Benkovic, S.J. "Bioorganic Mechanisms." Vol. II. New York: W.A. Benjamin, Inc., 1966:1–180.
89. Casareno, R.L.B., Li, D., Cowan, J.A. Rational redesign of a metal-dependent nuclease. Engineering the active site of magnesium-dependent ribonuclease H to form an active "metal-independent" enzyme. J. Am. Chem. Soc. 117:11011–11012, 1995.
90. Lohse, D.L., Denu, J.M., Santoro, N., Dixon, J.E. Roles of Asp-181 and Ser-222 in intermediate formation and hydrolysis of the mammalian protein phosphatase PTP1. Biochemistry 36:4568–4575, 1997.
91. Denu, J.M., Dixon, J.E. A catalytic mechanism for the dual-specific phosphatases. Proc. Natl. Acad. Sci. USA 92:5910–5914, 1995.